Performance evaluation of solar-PV integrated hybrid fuzzy-logic controlled multi-functional UPQC for enhancing PQ features

Lingineni Shanmukha Rao, Veera Narasimha Murthy Mogilicharla, Pidatala Prabhakara Sharma, Prathipati Rajkumar
Department of Electrical and Electronics Engineering, Kallam Haranadhareddy Institute of Technology, Guntur, India

Article Info

ABSTRACT

To improve distribution system voltage and current quality, a newly built solar-PV system connected multi-functional universal power quality compensator (MFUPQC) has been extensively used. The proposed MFUPQC mitigates both load and source-side concerns in a three-phase distribution system. Furthermore, as part of the distributed generation scheme, active power from solar PV is injected into the grid or source when solar PV is available. In this context, the proposed MFUPQC was tested in both PQ enhancement and DG integration modes using a feasible control scheme. The proportional-integral controller is used for shunt- voltage-source inverter (VSI) DC-link control, which is not suitable for regulating DC-link voltage at the desired level due to incorrect gain value selection. In this work, an intelligent hybrid-fuzzy-logic DC-link control of MFUPQC evidences the intelligent knowledge base for better regulation of power-quality issues. The suggested hybrid fuzzy-logic controlled MFUPQC device's performance for both power quality (PQ) improvement and DG integration is validated using the MATLAB/Simulink software tool, and simulation results are provided with an appealing comparison analysis.

Corresponding Author:

Lingineni Shanmukha Rao
Department of Electrical and Electronics Engineering, Kallam Haranadhareddy Institute of Technology
Guntur, Andhra Pradesh, India
Email: lsrlingineni@gmail.com

1. INTRODUCTION

Nowadays, electrical energy has grown into an essential part of modern society. The reliability and quality of electrical energy constitute key aspects in the secondary distribution system which is designed to meet the rated load demands. Millions of rupees are being spent to build power plants and transmission lines to satisfy the required load demand [1]. Numerous attempts have been taken around worldwide to promote the use of renewable energy for energy production named as distributed energy generation (DG) scheme [2]–[5]. Due to its ecologically friendly, virtuous, abundant nature, and noise-free characteristics, the solar-photovoltaic (PV) plays an important role in the DG-powered distribution system [6], [7]. During DG operations, absorbed solar energy is specifically connected to the common point (PCC) of the distribution network via power-electronic converters with an appropriate control system [8].

A number of constraints, including stable-flexible power supply, continuous support, and power-quality (PQ) norms, are required for the successful operation of DG schemes in distribution networks [9], [10]. Receiving quality power is a major consideration in secondary distribution systems due to the significant implications for users and utility-grid systems. It is expanding as a result of the widespread use of massive

power-electronic loads like industrial speed drives, switched-mode load apparatus, arc furnaces, heavy-inductive loads, and so on. The emergence of PQ issues causes critical issues in the distribution system, affecting supply terminal voltage, current, and fundamental frequency [11]. Poor power quality in the distribution system is mostly caused by supply voltage harmonics, sags-swells in supply voltage, current harmonics, unbalanced loads, low reactive power demand, and non-unity supply power factor, among other things [12], [13].

In fact, number of researchers and power engineers are being compelled to develop modern mitigation devices using custom-power technology (CPT) [14]–[18]. The UPQC is the most influential compensating device for resolving both current-voltage-related PQ problems, according to the literature [19]. The use of voltage-source inverter (VSI) elements built as a series-shunt constitute operated by a common DC capacitor for enhancing PQ in network is investigated in [20]. On the other hand, appears in a solar-PV-driven UPQC model for DG activity to control sudden-load variations [21]. Similarly, [22] looks into improving performance in DFIG-based wind-energy systems through the use of UPQC equipment and an advanced dual-control arrangement. The problem definition of previous works is carried from above studied literature, such as enhancing PQ; the addition of RES is more critical for maintaining grid norms by utilizing individual VSI operations, as discussed in [23], [24].

The proposed multi-functional universal power quality compensator (MFUPQC) device is composed of several VSIs coupled in series and driven by a single DC capacitor with the necessary voltage level for both PQ and DG operation modes. The proposed MFUPQC device requires reliable control algorithms that generate reference voltage and current signals from the source voltage and nonlinear load currents. In general, the synchronous reference frame (SRF) control theory [25] has been utilized to extract reference voltage to the MFUPQC device's series-VSI, and the instantaneous real-power (IRP) control theory [26] has been used to extract reference current to the MFUPQC device's shunt-VSI. Because of erroneous gain value selection, the proportional-integral controller is utilized for shunt-VSI DC-link control, which is not suitable for controlling DC-link voltage at the necessary level. In this work, an intelligent hybrid fuzzy-logic (HFL) DC-link control of MFUPQC evidences the intelligent knowledge base for better regulation of power-quality issues. The suggested hybrid fuzzy-logic controlled MFUPQC device's performance for both PQ improvement and DG integration is validated using the MATLAB/Simulink software tool, and simulation results are provided with an appealing comparison analysis.

2. PROPOSED CONCEPT

Figure 1 shows the block diagram representation of proposed MFUPQC device. For driving a non-linear unbalanced load through a three-phase 3-wire secondary distribution system, the proposed MFUPQC device is highly recommended. The designed solar-PV-connected MFUPQC is built in a series-shunt fashion to a distribution system for DG operation and also improving voltage and current quality.
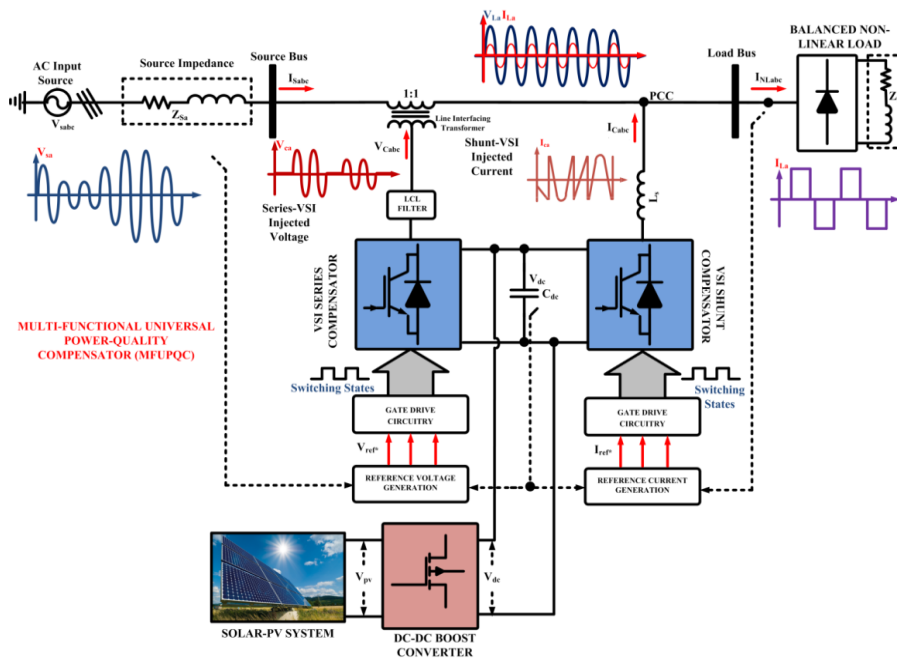

Figure 1. Block diagram representation of proposed multi-functional UPQC device

The MFUPQC comprises of dual-VSIs, control schemes, gate-drive system, DC-capacitor unit, and line interface filters. The MFUPQC device of shunt-VSI operates as shunt-connected active filtering in PQ improvement mode, it alleviating all current affiliated problems such as current harmonic distortions, load balancing, reactive-power control, and sustaining suitable power factor. The MFUPQC of shunt-VSI is integrated to PCC of the distribution system through external RL filters that eliminate inconsistent elements and notching impacts.

Similarly, the MFUPQC device of series-VSI operates as a series-connected active filtering to alleviate all voltage-affiliated problems such as voltage sag-swells, and balance of loads. The MFUPQC of series-VSI is coupled to the distribution system of PCC via a 1:1 line connected transformer with external RC filters that eliminate inconsistent notching impacts. The obtainable solar-PV power is supplied directly to the distribution system in DG operating mode in order to adjust the variations in load during the grid-isolation state.

It also reduces supply current usage when solar-PV power is available via a DC-DC boost converter; it achieves a high boost voltage, which is managed by an INC-MPPT control unit. Under fluctuating irradiance and temperature conditions, the INC-MPPT control unit maximizes power extraction from the solar-PV. The available solar PV power is transferred to the distribution system via the MFUPQC device's shunt-VSI, which is controlled by the IRP controller.

3.   CONTROL SCHEMES
3.1. IRP control for shunt-VSI of MFUPQC device

In most cases, the IRP controller is implemented as Clarke's conversion technique, which converts conventional abc into symmetrical coordinates in a stationary frame. The supply voltage Vst.abc and the distorted non-linear load currents INL.abc are translated into symmetrical frames for regulating both real and reactive powers as $(V_{st.\alpha\beta}, I_{NL.\alpha\beta})$. In (1) and (2), the Clarke's transformation process describes the supply voltages and non-linear load currents.

$$\begin{bmatrix} v_{st.\alpha} \\ v_{st.\beta} \end{bmatrix} = \sqrt{\frac{2}{3}} \begin{bmatrix} 1 & -1/2 & -1/2 \\ 0 & \sqrt{3}/2 & -\sqrt{3}/2 \end{bmatrix} \cdot \begin{bmatrix} v_{st.a} \\ v_{st.b} \\ v_{st.c} \end{bmatrix} \tag{1}$$

$$\begin{bmatrix} i_{NL.\alpha} \\ i_{NL.\beta} \end{bmatrix} = \sqrt{\frac{2}{3}} \begin{bmatrix} 1 & -1/2 & -1/2 \\ 0 & \sqrt{3}/2 & -\sqrt{3}/2 \end{bmatrix} \cdot \begin{bmatrix} i_{NL.a} \\ i_{NL.b} \\ i_{NL.c} \end{bmatrix} \tag{2}$$

The immediate values corresponding to the reactive and real powers in a symmetry frame are calculated using (1), (2), and (3), (4).

$$p = v_{st.\alpha} i_{NL.\alpha} + v_{st.\beta} i_{NL.\beta} \tag{3}$$

$$q = -v_{st.\beta} i_{NL.\alpha} + v_{st.\alpha} i_{NL.\beta} \tag{4}$$

In matrix form, the assessed power components are as:

$$\begin{bmatrix} p \\ q \end{bmatrix} = \begin{bmatrix} v_{st.\alpha} & v_{st.\beta} \\ -v_{st.\beta} & v_{st.\alpha} \end{bmatrix} \begin{bmatrix} i_{NL.\alpha} \\ i_{NL.\beta} \end{bmatrix} \tag{5}$$

The affected irregular load currents in the symmetry -frame are defined as:

$$\begin{bmatrix} i_{NL.\alpha} \\ i_{NL.\beta} \end{bmatrix} = \frac{1}{\Delta_k} \begin{bmatrix} v_{st.\alpha} & v_{st.\beta} \\ -v_{st.\beta} & v_{st.\alpha} \end{bmatrix} \begin{bmatrix} p \\ q \end{bmatrix} \tag{6}$$

where,

$$\Delta_k = v_{st.\alpha}^2 + v_{st.\beta}^2 \tag{7}$$

The resulting actual currents are then routed via a high-pass filtering process, allowing more complex components to get specific signals that serve as references. The high-frequency sections are treated, leading to a component loss denoted as ($P_{.Loss}$). Furthermore, by utilizing the right gains parameters of PI controller used in the DC control section, which is coupled to the primary controller, the DC voltage obtained from solar-PV of the shunt VSI remains continuously constant. The DC control section corrects errors induced by the variation

of the actual DC voltage $(V_{dc.a})$ and a reference DC voltage $(V_{dc.r}^*)$. As shown in (8) and (9) show the outcome of the controlling section at the nth point.

$$V_{dc.er} = V_{dc.r}^* - V_{dc.a} \tag{8}$$

$$\Delta_{ia.dc} = K_{p.d} * \left(V_{dc.er(n)} - V_{dc.er(n-1)}\right) + K_{i.d} * \left(V_{dc.er(n)}\right) \tag{9}$$

The performance of a PI controller is always dependent on the selection of feasible gains with necessary steps using the Ziegler Nichols method. Because of this method, the traditional PI controller does not auto-tune the gain values during parametric variations, sudden variations, and affecting the overall system stability. The significance of an intelligent HFL controller in symbolic characterization of an inference system with significant expert knowledge is realized. This HFL controller exemplifies the intelligent knowledge-based process with the combination of PI controller, which included FL-membership functions and a HFL-rule base [27]. The block diagram of HFL control scheme is depicted in Figure 2. These HFL-membership functions and HFL-rules are key components in HFL controller by incorporating significant human knowledge into an artificial knowledge base. Several attempts have been made to interpret the necessary enhancement in system performance by incorporating the superior learning technique to commute the HFL-rules and HFL-membership functions. The HFL-rule base is the heart of HFL control and the gathering of necessary information for depicting data manipulation values, linguistic models, and HFL-rule characterization, among other things [28]–[35].

$$e(s) = V_{dc.r}^* - V_{dc.a} \tag{10}$$

$$\Delta e(s) = e(s) - e(s-1) \tag{11}$$

Where, $e(s)$ and $\Delta e(s)$ are the error and change in error.

For feasible combinations obtained from HFL-input data, a look-up table related to discrete universes representation of HFL control outcome is developed. The fuzzy inference system provides information on how the FL controller performs certain logical operations in conjunction with the knowledge base as "IF, and Then" from various linguistic logic functions [36]. The HFL controller has a high robust performance, is model free, has a high strength index, and is operated as a subjective decision based on a universe-approximation technique with a HFL-rule base algorithm. The related HFL-membership functions and HFL-rule Base is clearly depicted in Table 1 and Figure 3.
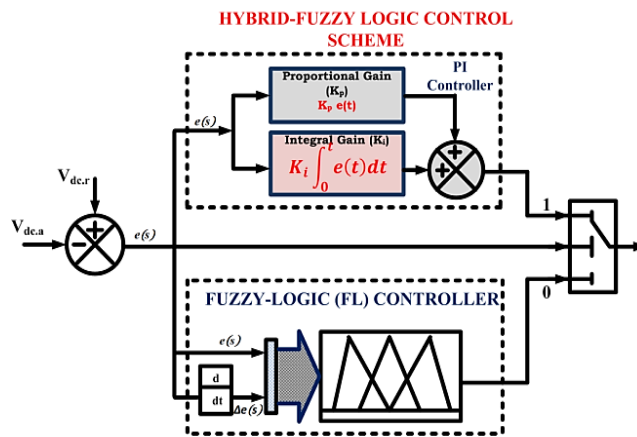

Figure 2. Block diagram of HFL controller

Table 1. HFL-rule-base

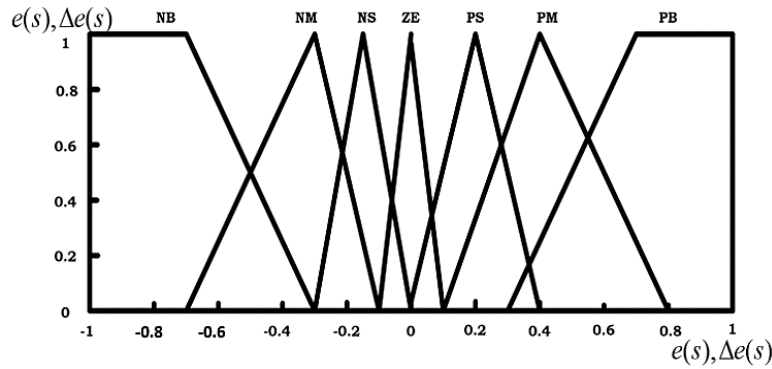| $e(s)$ / $\Delta e(s)$	NB	NM	NS	ZE	PS	PM	PB
NB	NB	NB	NB	NB	NM	NS	ZE
NM	NB	NB	NB	NM	NS	ZE	PS
NS	NB	NB	NM	NS	ZE	PS	PM
ZE	NB	NM	NS	ZE	PS	PM	PB
PS	NM	NS	ZE	PS	PM	PB	PB
PM	NS	ZE	PS	PM	PB	PB	PB
PB	ZE	NM	NS	ZE	PS	PM	PB

Figure 3. HFL membership functions

These DC oscillatory and AC averaged values can be used to represent these instantaneous components:

$$p = \bar{p} + \tilde{p}$$

$$q = \bar{q} + \tilde{q} \tag{12}$$

where, $\tilde{p}\tilde{q}$ denotes the oscillatory values of the AC, and $\bar{p}\bar{q}$ represents the average values of the DC. Furthermore, in the symmetrical frame, the retrieved reference current signal ($i^*_{cr.\alpha\beta}$) is described as (13).

$$\begin{bmatrix} i^*_{cr.\alpha} \\ i^*_{cr.\beta} \end{bmatrix} = \frac{1}{\Delta_k} \begin{bmatrix} v_{st.\alpha} & -v_{st.\beta} \\ v_{st.\beta} & v_{st.\alpha} \end{bmatrix} \begin{bmatrix} p \\ q \end{bmatrix} \tag{13}$$

Figure 4 depicts the schematic architecture of the proposed HFL-IRP controller. As a result, the acquired reference currents ($i^*_{cr.\alpha\beta}$) in the. $\alpha\beta$-frame are reverted into the initial abc frame by the inverse Clarke's conversion process, yielding the final reference current ($i^*_{cr.abc}$) as illustrated in (14).

$$\begin{bmatrix} i^*_{cr.a} \\ i^*_{cr.b} \\ i^*_{cr.c} \end{bmatrix} = \sqrt{\frac{2}{3}} \begin{bmatrix} 1/\sqrt{2} & 1 & 0 \\ 1/\sqrt{2} & -1/2 & \sqrt{3}/2 \\ 1/\sqrt{2} & -1/2 & -\sqrt{3}/2 \end{bmatrix} \begin{bmatrix} i^*_0 \\ i^*_{c.\alpha} \\ i^*_{c.\beta} \end{bmatrix} \tag{14}$$
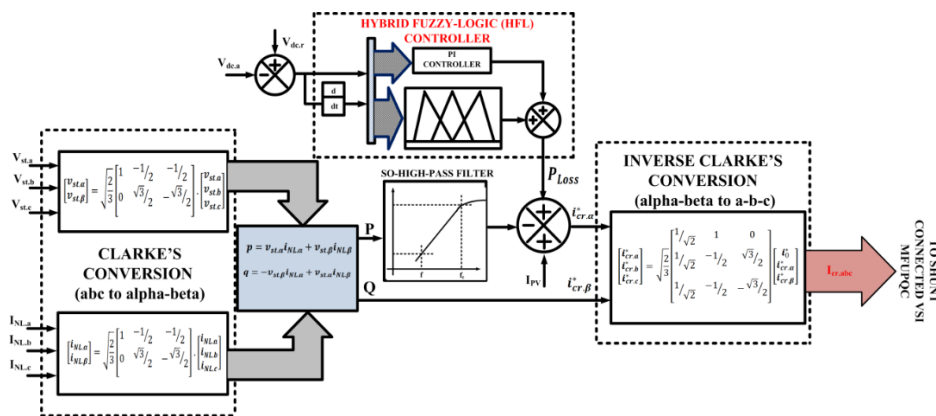

Figure 4. Schematic design of HFL-IRP control for shunt-VSI of MFUPQC device

3.2. SRF control of series-VSI of MFUPQC device

The MFUPQC of series-connected VSI is used to adjust for any voltage-related PQ concerns at the distribution system's PCC. The optimal operation of the MFUPQC's series-connected VSI is based on the

development of a reliable reference signal utilising an SRF controller with a sufficient supply voltage value. The precise supply voltage in an ordinary abc-frame (VL.abc) is turned into a spinning dq-frame (Vdq0.act) in a direct and quadrature axis using Park's conversion method.

$$\begin{bmatrix} V_{d.act} \\ V_{q.act} \\ V_{0.act} \end{bmatrix} = \frac{2}{3} \begin{bmatrix} cos\theta & cos\left[\theta - \frac{2\pi}{3}\right] & cos\left[\theta + \frac{2\pi}{3}\right] \\ sin\theta & sin\left[\theta - \frac{2\pi}{3}\right] & sin\left[\theta + \frac{2\pi}{3}\right] \\ \frac{1}{2} & \frac{1}{2} & \frac{1}{2} \end{bmatrix} \begin{bmatrix} V_{L.a} \\ V_{L.b} \\ V_{L.c} \end{bmatrix} \tag{15}$$

$$\theta = \int \omega . dt \tag{16}$$

Where θ denotes the displacement factor, ω denotes the angular velocity, VL.abc is the precise load voltage in the conventional abc frame, and Vdq0.abc, respectively, is the converted voltage for direct and quadrature frames. While functioning, the voltage that acts as a reference is kept constant, and the values of the dq-frame stay constant at 1 p.u. and 0 p.u. After the conversion, the real voltage (Vdq.act) may be separated from the reference voltage (Vdq.ref) to provide good compensation voltages as well as specific error sequences. These sequences are decreased by using a PI controller with correctly calibrated proportional (Kpa) and integral (Kia) gain levels. The transfer function of the PI controller is as:

$$U_{err}(s) = k_{pa} + \frac{k_{ia}}{s} E_{err}(s) \tag{17}$$

The schematic design of the SRF control of MFUPQC's series-connected VSI is shown in Figure 5. The PI controller's output is interpreted as a voltage reference signal (V_(dq.ref)*) since the error sequences are minimised. The corresponding signals in the dq-frame are then re-converted into the precise ABC using the inverse-Park's conversion approach, as given in (18).

$$V_{dq.ref}^* = (V_{dq.ref} - V_{dq.act}) \tag{18}$$

$$\begin{bmatrix} V_{a.ref} \\ V_{b.ref} \\ V_{c.ref} \end{bmatrix} = \frac{2}{3} \begin{bmatrix} cos\theta & sin\theta & 1 \\ cos\left[\theta - \frac{2\pi}{3}\right] & sin\left[\theta - \frac{2\pi}{3}\right] & 1 \\ cos\left[\theta + \frac{2\pi}{3}\right] & sin\left[\theta + \frac{2\pi}{3}\right] & 1 \end{bmatrix} \begin{bmatrix} V_{d.ref}^* \\ V_{q.ref}^* \end{bmatrix} \tag{19}$$

Finally, utilising hysteresis current control (HCC) and sinusoidal pulse-width modulation (PWM), the calculated reference currents and voltages from FL-IRP/SRF controllers are contrasted with accurate basic values for the creation of switching conditions to shunt and series VSIs of MFUPQC. The suggested HFL controlled MFUPQC device's performance for both PQ improvement and DG integration is validated using the MATLAB/Simulink software tool, and simulation results are provided with an appealing comparison analysis. The system data is presented in Table 2.
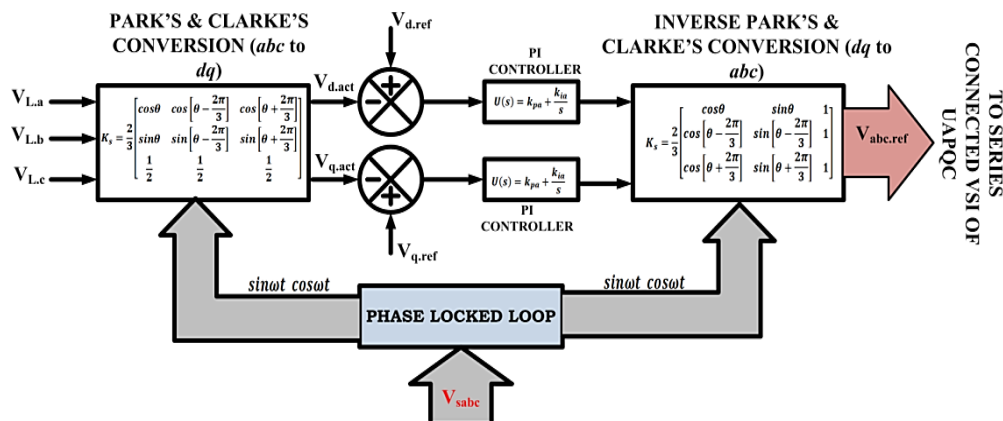

Figure 5. Schematic design of SRF controller for series-connected VSI of MFUPQC

Table 2. System data

S. No	System Data	Values
1	Supply voltage	V_{sabc}-415 V, F_S-50 Hz
2	Supply impedance	Rs-0.1 Ω, Ls-0.9 mH
3	Non-linear load impedance	R_{NL}-20 Ω, L_{NL}-30 mH
4	DC capacitor	V_{dc}-880 V, C_{dc}-1500 μF
5	VSI's Filter	R_f-0.1 Ω, L_f-5 mH
6	Solar-PV values	V_{pv}-400 V, I_{pv}-50 A, P_{pv}-20 KW
7	PI controller	K_p-18.3, K_i-4.3

4.   MATLAB/SIMULINK RESULTS AND DISCUSSION
4.1. Power-quality enhancement using proposed hybrid-fuzzy logic-controlled IRP Driven MFUPQC device

Figure 6 depict harmonic current reduction in a three-phase distribution system employing an HFL driven shunt linked VSI of an MFUPQC device. For driving the non-linear unbalanced load, the three-phase distribution system is powered by a three-phase supply voltage of Vrms-415 V and a rated frequency of Fs-50 Hz. The three-phase diode-bridge rectifier with uneven impedance of the load has been regarded as an unbalanced non-linear load, introducing harmonic unbalanced currents that proliferate the current quality at the distribution system's PCC. The non-linear imbalanced load uses almost the rated current nearly 36 A which distorts the supply or PCC current which generates more heat loss and damaging the other nearby connected loads at PCC level. A shunt-connected VSI of an MFUPQC device controlled by an HFL-controlled IRP controller is utilized to decrease current harmonics at the PCC. It injects the appropriate in-phase compensatory currents that compensate for the 38 A supply current's harmonics and imbalance nature.
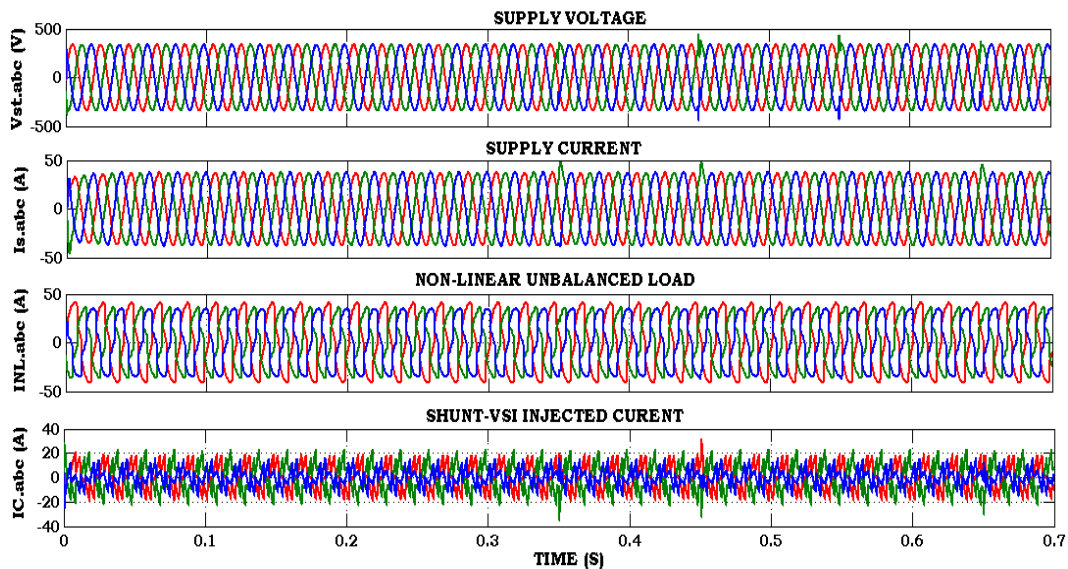

Figure 6. Mitigation of harmonic currents

The sinusoidal in shape, simple, fundamental, balanced power supply or PCC current is subsequently generated by the MFUPQC device's shunt connected VSI. The supply or PCC current is in phase with the supply or PCC voltage, as shown in Figure 7, resulting in a power-factor of unity at the supply or PCC level. The observed total harmonic distortion (THD) of non-linear unbalanced load current is 21.77%, while the observed THD of supply current is 1.77%, as shown in Figures 8 and 9, suggesting that the THD values of supply current are within IEEE-519/2014 guidelines.

The voltage sags-swells mitigation employing series linked VSI of MFUPQC device in a distribution network is shown in Figure 10. For driving the non-linear unbalanced load, the three-phase distribution system is powered by a supply with a three-phase voltage of Vrms-415 V and a standard frequency of Fs-50 Hz. In this circumstance, voltage sags-swells arise from the supply voltage, influencing the imbalanced nonlinear load and propagating the electrical voltage quality at the distribution system's PCC. To relieve voltage sags-swells, the MFUPQC device's series-connected VSI balances the sags-swells in load voltage, resulting in a balanced, steady, and sinusoidal load or PCC voltage.
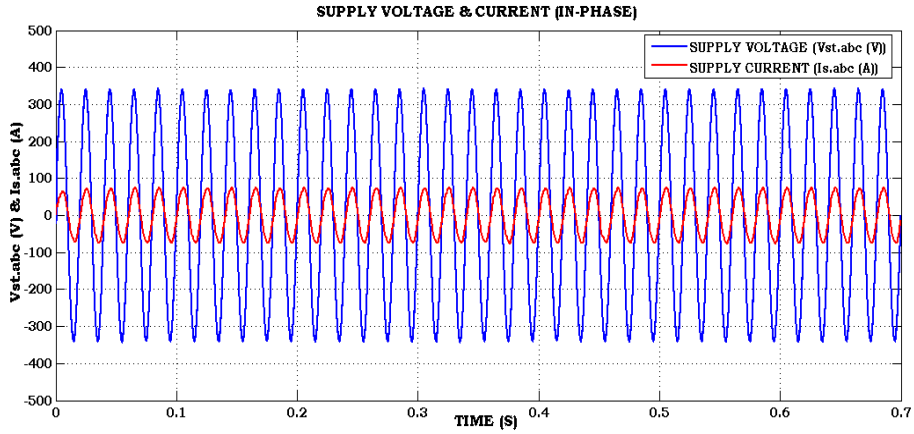
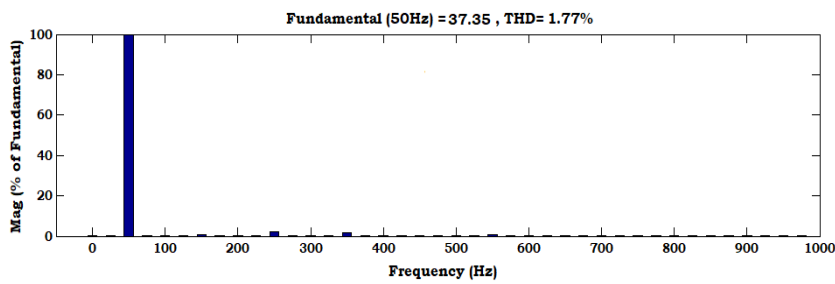Figure 7. In-phase of supply voltage and current

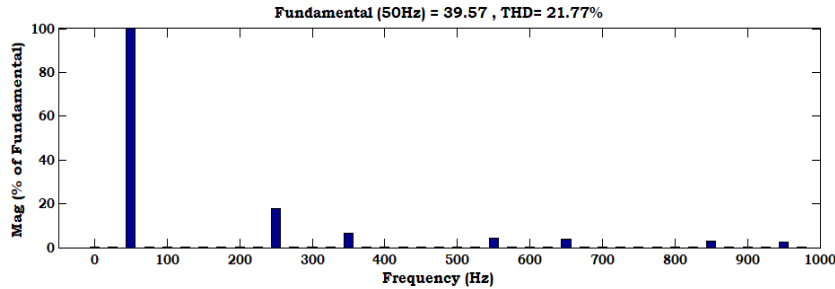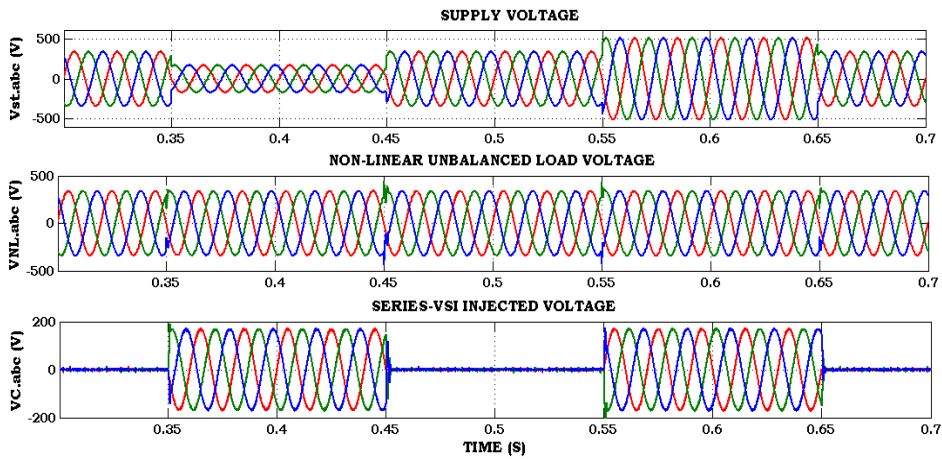Figure 8. THD value of non-linear load current

Figure 9. THD value of supply current

Figure 10. Mitigation of voltage sag and swells using series VSI of MFUPQC device

During the time t-(0<t<0.35 sec) believed to be the pre-sag condition, the supply voltage is kept constant at 340 V. During the time t-(0.35<t<0.45 sec), the voltage-sag appears, and the supply voltage is dropped by 50%, compromising the continuous functioning of the non-linear unbalanced load. In this time state, the MFUPQC device's series linked VSI injects the required voltage of 170 V, causing the non-linear load voltage to remain constant at 340 V. During the time t-(0.55<t<0.65 sec), the voltage-swell appears, and the supply voltage rises by 50%, disrupting the continuous functioning of the non-linear imbalanced load. In this time state, the MFUPQC device's series linked VSI extracts an additional voltage of 170 V, causing the non-linear load voltage to remain constant at 340 V.

4.2. A solar-PV integrated distribution system using proposed hybrid-fuzzy logic-controlled IRP driven MFUPQC device

Figure 11 depict the simulation results of a solar-PV integrated distribution system employing the proposed hybrid-fuzzy logic-controlled IRP driven MFUPQC device. It consists of Figure 11(a) supply specifications for DG integration, Figure 11(b) solar-PV voltage, solar-PV power, and DC-link voltage, in that order. For powering the non-linear imbalanced load, the three-phase distribution network is powered by a supply with a three-phase voltage of Vrms-415 V and a nominal frequency of Fs-50 Hz. In this case, the acquired solar-PV energy is sent to the distribution system via the MFUPQC device's shunt-connected VSI for active-power exchange during block-outs and grid-isolation mode. When solar-PV power is available, the system delivers available solar power to load which reduces the power consumption from utility-grid or main source, then the value of supply current is reducing based on availability of solar-PV energy as shown in Figure 11(a). The generated solar-PV energy is boosting up to high voltage by using DC-DC boost converter which is regulated by INC-MPPT control algorithm.
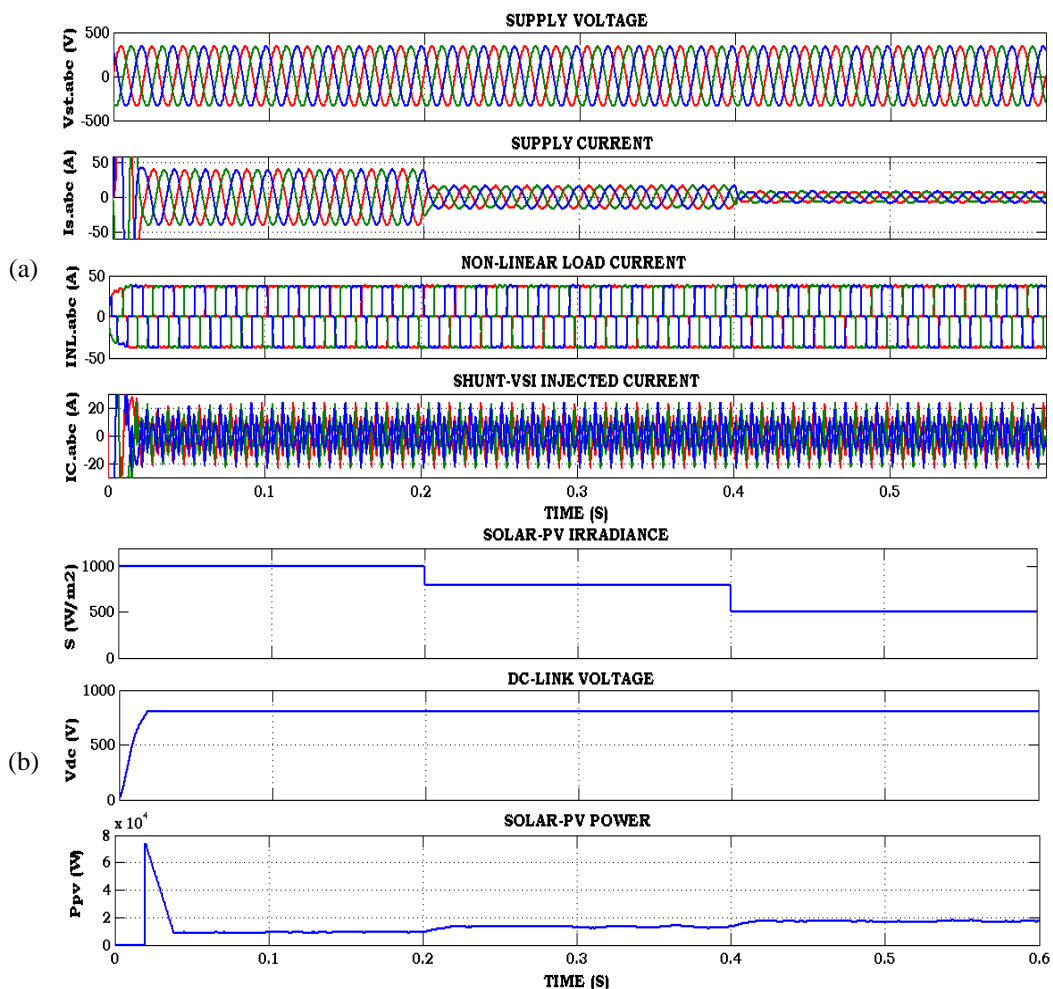

Figure 11. Solar-PV integrated distribution network using proposed hybrid-fuzzy logic-controlled IRP driven MFUPQC device (a) supply specifications and (b) solar-PV voltage, solar-PV power and DC-link voltage

The INC-MPPT algorithm extracts the solar-PV maximum power when variable irradiance and temperature conditions. The irradiance level is slightly varied with a value of 1000 W/m^2 to 800 W/m^2 during the time instant t-(0<t<0.2 sec). And also varies with a value of 800 W/500 W m^2 to /m^2 during the time instant t-(0.2<t<0.4 sec). Therefore, the obtained solar-PV energy is also varies along with variable irradiance and the injected current in to PCC of distribution system is also varies, but the DC-link voltage is regulated as constant with a value of 880 V is shown in Figure 11(b). The comparisons of non-linear unbalanced load current THD's and supply currents THD's of conventional PI-IRP, fuzzy-IRP and proposed hybrid-fuzzy IRP controlled MFUPQC device are illustrated in Table 3 and graphical view is depicted in Figure 12. Among the conventional PI-IRP and fuzzy-IRP control performance, the proposed hybrid-fuzzy controlled IRP controller driven MFUPQC device has better harmonic reduction which increases the stable performance and better enhancement of power-quality features.
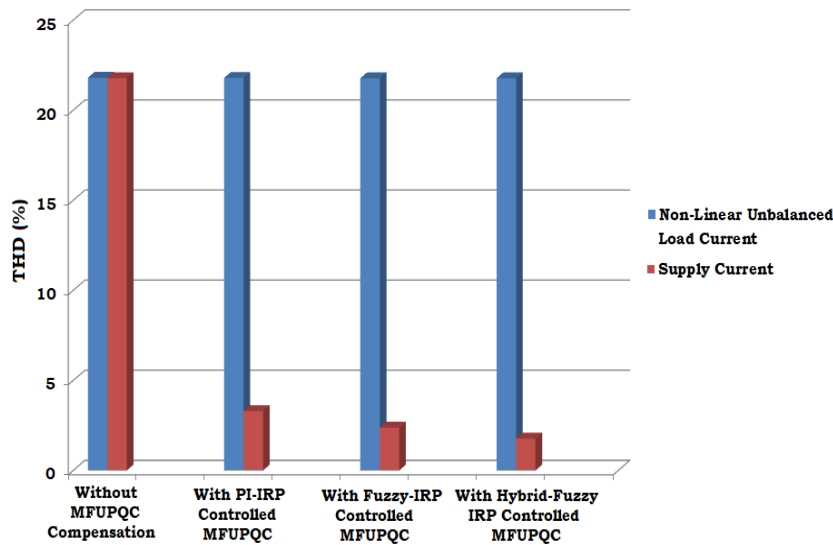

Figure 12. Graphical view of THD comparisons in conventional PI-IRP, FL-IRP and proposed hybrid-fuzzy IRP controlled MFUPQC device

Table 3. Comparisons of non-linear unbalanced load current THD's and supply currents THD's of conventional PI-IRP, fuzzy-IRP and proposed hybrid-fuzzy IRP controlled MFUPQC device

THD (%)	Non-linear unbalanced load current	Supply current
Without MFUPQC compensation	21.80%	21.78%
With PI-IRP controlled MFUPQC	21.79%	3.30%
With fuzzy-IRP controlled MFUPQC	21.77%	2.38%
With HFL-IRP controlled MFUPQC	21.77%	1.77%

5. CONCLUSION

In this work, an attractive solar-PV driven DG connected distributed system for delivering the requisite load demand complying with enhanced power-quality by using proposed Hybrid-Fuzzy IRP controlled MFUPQC device. The Hybrid-Fuzzy IRP controlled MFUPQC enhances voltage and current quality in a PCC of distribution system with high stable performance and better compensation features in PQ mode over the conventional PI-IRP and FL-IRP control schemes. During abrupt load fluctuations, block-outs, and grid-isolation mode, the MFUPQC device's shunt linked VSI exchanges both reactive and active power. It also reduces supply current use during DG mode; the needed load power is met by solar-PV power. The measured THD value of non-linear unbalanced load current is 21.77%, while the measured THD value of supply current is 1.77%, indicating that supply current THD values are within IEEE-519/2014 norms.

REFERENCES

[1]   S. Nagaballi and V. S. Kale, "Impact of DG and D-STATCOM integration in RDN on power losses and voltage profile considering load growth," in *INDICON 2022 - 2022 IEEE 19th India Council International Conference*, Nov. 2022, pp. 1–6, doi: 10.1109/INDICON56171.2022.10039696.

[2]   L. Xuefeng, L. Kaiju, L. Weiqiang, M. Chaoxu, and W. Dan, "A brief analysis of distributed generation connected to distribution network," in *Proceedings - 2018 33rd Youth Academic Annual Conference of Chinese Association of Automation, YAC 2018*, May 2018, pp. 795–799, doi: 10.1109/YAC.2018.8406479.

[3]   G. Vikash, A. Ghosh, and S. Rudra, "Integration of distributed generation to microgrid with virtual inertia," in *2020 IEEE 17th India Council International Conference, INDICON 2020*, Dec. 2020, pp. 1–6, doi: 10.1109/INDICON49873.2020.9342377.

[4]   K. Vinothkumar and M. P. Selvan, "DG planning method for enhancement of voltage stability margin in distribution system," in *PEDES 2012 - IEEE International Conference on Power Electronics, Drives and Energy Systems*, Dec. 2012, pp. 1–6, doi: 10.1109/PEDES.2012.6484414.

[5]   J. Xiong, S. Liu, X. Wang, S. Zhu, J. Zheng, and K. Meng, "A stability enhancement method for inverter-based distributed generation systems," in *IEEE Power and Energy Society General Meeting*, Jul. 2015, vol. 2015-September, pp. 1–4, doi: 10.1109/PESGM.2015.7285737.

[6]   J. Sridevi, V. U. Rani, and B. L. Rao, "Integration of renewable DGs to radial distribution system for loss reduction and voltage profile improvement," in *2019 IEEE International Conference on Electrical, Control and Instrumentation Engineering, ICECIE 2019 - Proceedings*, Nov. 2019, pp. 1–6, doi: 10.1109/ICECIE47765.2019.8974670.

[7]   M. Shafiullah, S. D. Ahmed, and F. A. Al-Sulaiman, "Grid integration challenges and solution strategies for solar PV systems: a review," *IEEE Access*, vol. 10, pp. 52233–52257, 2022, doi: 10.1109/ACCESS.2022.3174555.

[8]   R. Panigrahi, S. K. Mishra, and S. C. Srivastava, "Grid integration of small-scale photovoltaic systems-a review," in *2018 IEEE Industry Applications Society Annual Meeting (IAS)*, Sep. 2018, pp. 1–8, doi: 10.1109/IAS.2018.8544503.

[9]   B. Banfield, P. Ciufo, and D. A. Robinson, "The technical and economic benefits of utility sponsored renewable energy integration," in *2017 Australasian Universities Power Engineering Conference, AUPEC 2017*, Nov. 2018, vol. 2017-November, pp. 1–6, doi: 10.1109/AUPEC.2017.8282489.

[10] K. Moloi, Y. Hamam, and J. A. Jordaan, "Optimal location of DGs into the power distribution grid for voltage and power improvement," in *2020 IEEE PES/IAS PowerAfrica, PowerAfrica 2020*, Aug. 2020, pp. 1–5, doi: 10.1109/PowerAfrica49420.2020.9219938.

[11] X. P. Zhang and Z. Yan, "Energy quality: a definition," *IEEE Open Access Journal of Power and Energy*, vol. 7, pp. 430–440, 2020, doi: 10.1109/OAJPE.2020.3029767.

[12] J. Yaghoobi, A. Abdullah, D. Kumar, F. Zare, and H. Soltani, "Power quality issues of distorted and weak distribution networks in mining industry: a review," *IEEE Access*, vol. 7, pp. 162500–162518, 2019, doi: 10.1109/ACCESS.2019.2950911.

[13] T. Tarasiuk *et al.*, "Review of power quality issues in maritime microgrids," *IEEE Access*, vol. 9, pp. 81798–81817, 2021, doi: 10.1109/ACCESS.2021.3086000.

[14] S. Singh and S. S. Letha, "Various custom power devices for power quality improvement: a review," in *2018 International Conference on Power Energy, Environment and Intelligent Control, PEEIC 2018*, Apr. 2018, pp. 689–695, doi: 10.1109/PEEIC.2018.8665470.

[15] E. Hossain, M. R. Tur, S. Padmanaban, S. Ay, and I. Khan, "Analysis and mitigation of power quality issues in distributed generation systems using custom power devices," *IEEE Access*, vol. 6, pp. 16816–16833, 2018, doi: 10.1109/ACCESS.2018.2814981.

[16] T. A. Kumar and L. S. Rao, "Improvement of power quality of distribution system using ANN-LMBNN based D-STATCOM," in *2017 Innovations in Power and Advanced Computing Technologies (i-PACT)*, Apr. 2017, vol. 2017-Janua, pp. 1–6, doi: 10.1109/IPACT.2017.8245211.

[17] J. V. Lakshmi* and L. S. Rao, "Power quality improvement using intelligent fuzzy-VLLMS based shunt active filter," *International Journal of Recent Technology and Engineering (IJRTE)*, vol. 8, no. 6, pp. 1004–1012, Mar. 2020, doi: 10.35940/ijrte.f7372.038620.

[18] T. Ganesh* and L. S. Rao, "Performance analysis of plug-in electric vehicle supported DVR for power-quality improvement and energy back-up strategy," *International Journal of Recent Technology and Engineering (IJRTE)*, vol. 8, no. 6, pp. 945–952, Mar. 2020, doi: 10.35940/ijrte.f7373.038620.

[19] S. S. N. L. Bhavani and L. Shanmukha Rao, "Realization of novel multi-feeder UPQC for power quality enhancement using proposed hybrid fuzzy+PI controller," in *2019 Innovations in Power and Advanced Computing Technologies, i-PACT 2019*, Mar. 2019, pp. 1–8, doi: 10.1109/i-PACT44901.2019.8960156.

[20] P. Ray, P. K. Ray, and S. K. Dash, "Power quality enhancement and power flow analysis of a PV integrated UPQC system in a distribution network," *IEEE Transactions on Industry Applications*, vol. 58, no. 1, pp. 201–211, Jan. 2022, doi: 10.1109/TIA.2021.3131404.

[21] K. Sarita *et al.*, "Power enhancement with grid stabilization of renewable energy-based generation system using UPQC-FLC-EVA technique," *IEEE Access*, vol. 8, pp. 207443–207464, 2020, doi: 10.1109/ACCESS.2020.3038313.

[22] R. H. Yang and J. X. Jin, "Unified power quality conditioner with advanced dual control for performance improvement of dfig-based wind farm," *IEEE Transactions on Sustainable Energy*, vol. 12, no. 1, pp. 116–126, Jan. 2021, doi: 10.1109/TSTE.2020.2985161.

[23] M. Prasad, Y. K. Nayak, R. R. Shukla, R. Peesapati, and S. Mehera, "Design and analysis of renewable-energy-fed UPQC for power quality improvement," in *Planning of Hybrid Renewable Energy Systems, Electric Vehicles and Microgrid Energy Systems in Electrical Engineering*, Springer, 2022, pp. 107–124.

[24] Y. R. Babu and C. S. Rao, "Analysis of grid tied distributed generation and power quality enhancement using dual SAPF," in *2017 International Conference on Energy, Communication, Data Analytics and Soft Computing, ICECDS 2017*, Aug. 2018, pp. 907–915, doi: 10.1109/ICECDS.2017.8389568.

[25] M. Kesler and E. Ozdemir, "Synchronous-reference-frame-based control method for UPQC under unbalanced and distorted load conditions," *IEEE Transactions on Industrial Electronics*, vol. 58, no. 9, pp. 3967–3975, Sep. 2011, doi: 10.1109/TIE.2010.2100330.

[26] K. Palanisamy, J. S. Mishra, I. J. Raglend, and D. P. Kothari, "Instantaneous power theory based unified power quality conditioner (UPQC)," in *2010 Joint International Conference on Power Electronics, Drives and Energy Systems, PEDES 2010 and 2010 Power India*, Dec. 2010, pp. 1–5, doi: 10.1109/PEDES.5712453.

[27] G. Satyanarayana, K. N. V. Prasad, G. R. Kumar, and K. L. Ganesh, "Improvement of power quality by using hybrid fuzzy controlled based IPQC at various load conditions," in *2013 International Conference on Energy Efficient Technologies for Sustainability*, Apr. 2013, pp. 1243–1250, doi: 10.1109/ICEETS.2013.6533565.

[28] G. Satyanarayana and K. Lakshmi Ganesh, "Tuning a robust performance of adaptive fuzzy-PI driven DSTATCOM for non-linear process applications," in *Lecture Notes in Computer Science (including subseries Lecture Notes in Artificial Intelligence and Lecture Notes in Bioinformatics)*, vol. 8947, 2015, pp. 523–533.

[29] Y. M. Esmail, A. H. Kasem Alaboudy, M. S. Hassan, and G. M. Dousoky, "Mitigating power quality disturbances in smart grid using FACTS," *Indonesian Journal of Electrical Engineering and Computer Science (IJEECS)*, vol. 22, no. 3, pp. 1223–1235, Jun. 2021, doi: 10.11591/ijeecs.v22.i3.pp1223-1235.

[30] L. Hichem, O. Amar, and M. Leila, "Optimized ANN-fuzzy MPPT controller for a stand-alone PV system under fast-changing atmospheric conditions," *Bulletin of Electrical Engineering and Informatics (BEEI)*, vol. 12, no. 4, pp. 1960–1981, Aug. 2023, doi: 10.11591/eei.v12i4.5099.

[31] J. Kaur and A. Khosla, "Simulation and harmonic analysis of hybrid distributed energy generation based microgrid system using intelligent technique," *Indonesian Journal of Electrical Engineering and Computer Science (IJEECS)*, vol. 30, no. 3, pp. 1287–1296, Jun. 2023, doi: 10.11591/ijeecs.v30.i3.pp1287-1296.

[32] S. N. Setty, M. S. D. Shashikala, and K. T. Veeramanju, "Hybrid control mechanism-based DVR for mitigation of voltage sag and swell in solar PV-based IEEE 33 bus system," *International Journal of Power Electronics and Drive Systems (IJPEDS)*, vol. 14, no. 1, pp. 209–221, Mar. 2023, doi: 10.11591/ijpeds.v14.i1.pp209-221.

[33] I. Abadi, A. Musyafa, K. G. Erwandha, and D. N. Fitriyanah, "Design and building of a battery charging system using hybrid solar tracker and electric trip based on FPAO-FLC," *International Journal of Power Electronics and Drive Systems (IJPEDS)*, vol. 13, no. 4, pp. 2305–2312, Dec. 2022, doi: 10.11591/ijpeds.v13.i4.pp2305-2312.

[34] V. S. Sree and C. Srinivasa Rao, "Distributed power flow controller based on fuzzy-logic controller for solar-wind energy hybrid system," *International Journal of Power Electronics and Drive Systems (IJPEDS)*, vol. 13, no. 4, pp. 2148–2158, Dec. 2022, doi: 10.11591/ijpeds.v13.i4.pp2148-2158.

[35] A. Ibnelouad, A. Elkari, H. Ayad, and M. Mjahed, "A neuro-fuzzy approach for tracking maximum power point of photovoltaic solar system," *International Journal of Power Electronics and Drive Systems*, vol. 12, no. 2, pp. 1252–1264, Jun. 2021, doi: 10.11591/ijpeds.v12.i2.pp1252-1264.

[36] M. Nagaiah and K. C. Sekhar, "Analysis of fuzzy logic controller based bi-directional DC-DC converter for battery energy management in hybrid solar/wind micro grid system," *International Journal of Electrical and Computer Engineering (IJECE)*, vol. 10, no. 3, pp. 2271–2284, Jun. 2020, doi: 10.11591/ijece.v10i3.pp2271-2284.

BIOGRAPHIES OF AUTHORS

Lingineni Shanmukha Rao received Ph.D. from Jawaharlal Nehru Technological University Hyderabad (JNTUH), Hyderabad, India in 2016 and M.Tech. in electrical power engineering from Jawaharlal Nehru Technological University (J.N.T.U), Hyderabad, A.P, India in 2006. At present he is working as Professor and Head of the Department Electrical and Electronics Engineering at Kallam Haranadhareddy Institute of Engineering and Technology, Guntur, A.P., India. He authored four books and published more than 25 research papers in international journals and conferences. His research interests include power system modeling and control, renewable energy sources, and soft computing techniques. He can be contacted at email: lsrlingineni@gmail.com.

Veera Narasimha Murthy Mogilicharla obtained his B.Tech. in EEE from Narasaraopeta Engineering College, Andhra Pradesh, India. He completed Master of Technology in Electrical Power Systems from University college of Engineering JNTUA-University. He is pursuing Ph.D. from Acharya Nagarjuna University, Guntur, India. His area of interest includes electrical power systems, renewable energy sources, power quality issues, and FACTS devices. He can be contacted at email: murthyeps@gmail.com.

Pidatala Prabhakara Sharma received obtained his B.Tech. in EEE from KLCE, AP, India. He completed his Master of Technology in High Voltage Engineering from University College of Engineering, JNTUK- Kakinada. AP, India and pursing Ph.D. in Andhra University. He is currently working as Associate Professor in Electrical & Electronics Engineering Department in Kallam Haranadhareddy Institute of Technology, Guntur, AP, India, since 2013. He published more than 20 papers in international journals and conferences. He filed three patents. His area of interest includes electrical machines, HVDC, AC-DC power flows, and soft computing techniques. He can be contacted at email: prabhakarasharma@gmail.com.

Prathipati Rajkumar is an Under Graduate student studying IV B.Tech. electrical and electronics engineering from Kallam Haranadhareddy Institute of Engineering and Technology, Guntur, A.P., India. He is one of the topper at the college level who got meritorious scholarship and won many prizes in the technical events held at intra and inter college level. His research interests include renewable energy sources. He can be contacted at email: rajprathipati9@gmail.com.